POLITECNICO DI TORINO
Repository ISTITUZIONALE

Performance Assessment of Ferrite-Assisted Synchronous Reluctance Motors for Traction Applications

Original
Performance Assessment of Ferrite-Assisted Synchronous Reluctance Motors for Traction Applications / Ferrari, Simone; Dilevrano, Gaetano; Bergsro, Kim; Bertoncello, Tommaso; Pellegrino, Gianmario. - ELETTRONICO. - (2024), pp. 1-7. (Intervento presentato al convegno 2024 International Conference on Electrical Machines (ICEM) tenutosi a Torino nel 01-04 September 2024) [10.1109/icem60801.2024.10700381].

Availability:
This version is available at: 11583/2993315 since: 2024-10-10T20:57:41Z

Publisher:
IEEE

Published
DOI:10.1109/icem60801.2024.10700381

Terms of use:

This article is made available under terms and conditions as specified in the corresponding bibliographic description in the repository

Publisher copyright
IEEE postprint/Author's Accepted Manuscript

©2024 IEEE. Personal use of this material is permitted. Permission from IEEE must be obtained for all other uses, in any current or future media, including reprinting/republishing this material for advertising or promotional purposes, creating new collecting works, for resale or lists, or reuse of any copyrighted component of this work in other works.

(Article begins on next page)

03 January 2025

Performance Assessment of Ferrite-Assisted Synchronous Reluctance Motors for Traction Applications

Simone Ferrari
Energy Department "Galileo Ferraris"
Politecnico di Torino
Turin, Italy
simone.ferrari@polito.it

Gaetano Dilevrano
Energy Department "Galileo Ferraris"
Politecnico di Torino
Turin, Italy
gaetano.dilevrano@polito.it

Kim Bergsro
Electric Driveline Department
Volvo Cars Corporation
Gothenburg, Sweden
kim.bergsro@volvocars.com

Tommaso Bertoncello
Electric Driveline Department
Volvo Cars Corporation
Gothenburg, Sweden
tommaso.bertoncello@volvocars.com

Gianmario Pellegrino
Energy Department "Galileo Ferraris"
Politecnico di Torino
Turin, Italy
gianmario.pellegrino@polito.it

***Abstract*—The paper presents a feasibility study on Synchronous Reluctance motors with and without the assistance of ferrite permanent magnets in the field of traction application. Three prototypes with slightly different specification will be compared in terms of electromagnetic performance figures, considering the effect on key performance indicators of the initial design choices and constraints. An example of permanent magnet motor with rare-earth magnets is selected as reference, to enhance the pros and cons of the rare-earth-free solutions. Furthermore, the environmental impact of the four motors will be considered, both in general terms and through specific indicators.**

***Index Terms*—Synchronous Reluctance Motors, Traction Application, Ferrite-assisted Synchronous Reluctance Motor**

I. Introduction

Electric vehicle (EV) sector experiments a huge development in the last decades, mainly because of the need of a more efficient mobility solution with lower environmental impact than the standard vehicles with internal combustion engine. The majority of electric motors for EVs are Permanent Magnets Synchronous Motors (PMSMs) [1], because of their superior torque and power density compared to other electrical machines. Furthermore, anisotropic rotor structures can be adopted, further improving the power density and allowing efficient field-weakening operations and the inverter rating reduction, covering all the possible vehicle operations [2]. The last trend goes in the direction of increase the maximum speed of traction motors [3], [4], allowing an even more higher power density, at the cost of a more critical structural and magnetic design. Indeed, to reach high speed (10-20 krpm or more), the rotor shape must be optimized to sustain the high centrifugal stress, with a detriment of the magnetic properties. Besides the higher efficiency of the electric powertrains compared to the internal combustion engine systems, due to the absence of the combustion, the environmental impact of EVs must be assessed in a critical way, since some of the materials adopted in the electric motors have a huge environmental impact. One of the most critical materials on an environmental point of view are the Permanent Magnets (PMs). Typically, NdFeB magnets are adopted. These PMs offer high energy, high remanence and low risk of demagnetization (except for high temperatures and severe fault scenarios), at the cost of high environmental impact. However, thanks to the high power density guaranteed, NdFeB-based PMSMs are the standard in the automotive sector. A possible alternative to the NdFeB is the use of weak ferrite magnets for the PMSMs, together with a high-anisitropic geometry, typical of the Symchronous Reluctance Motors (SyRMs) [5]. These ferrite PMs presents about 1/3 to 1/4 of the remanence of the NdFeB PMs and a low resistance against irreversible demagnetization (especially at cold temperatures), but have an environmental impact that is about 200 times lower compared to NdFeB PMs [6]. In the following, four electric motors for traction applications are compared in terms of specific performance indexes, that account both for the electromagnetic performance and the environmental impact. Per-unit factors will be adopted to make the comparison as fair as possible. The cross-sections of the four motors are reported in Fig. 1 and their main specifications are reported in Tab. I in per-unit of Mot1 specs. Among the four motors, two of them (Mot1 and Mot3) are PM-SyRMs with ferrite PMs, one (Mot2) is a pure SyRM, that employ the same stator lamination of Mot1 and the last is a NdFeB PMSM with V-type barrier. The former three motors are prototypes designed on purpose, while the latter is reconstructed from an product already adopted in commercial vehicles [7]. The four motors have slightly different target performance, both in terms of torque and maximum speed, that affects the rotor design. Furthermore, the inverters adopted for the three motor

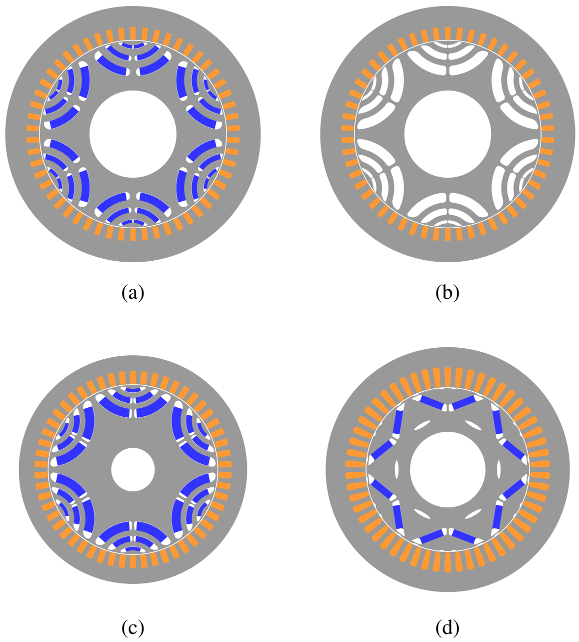

Fig. 1. Cross section of the four considered prototypes: Mot1 and Mot3 have ferrite PMs while Mot4 have NdFeB PMs.

TABLE I
SPECS COMPARISON

	Mot1	**Mot2**	**Mot3**	**Mot4**
Rotor type	PM-SyR	SyR	PM-SyR	V-type
PM type	ferrite	-	ferrite	NdFeB
Number of poles	6	6	6	6
Number of stator slots	54	54	54	54
Stator outer diameter	1.00	1.00	0.89	0.96
Stack length	0.77	0.49	0.62	0.57
Rotor outer diameter	0.73	0.73	0.66	0.64
Peak torque	1.00	0.62	0.81	0.95
Peak power	1.00	0.64	0.61	0.70
Base speed	0.34	0.35	0.25	0.25
Maximum speed	1.00	0.84	0.64	0.91
Power at max speed	0.43	0.18	0.35	0.58
Peak phase current	1.00	0.80	0.86	1.01
DC-link voltage	1.00	1.00	0.71	0.58
Inverter rating	1.00	0.80	0.61	0.59
Active mass	1.00	0.59	0.61	0.70
Active volume	1.00	0.64	0.64	0.68

are different. Dealing with the windings, the first three motors have hairpin windings, while Mot4 is has stranded winding. The results reported in the following are computed with Finite Elements Analysis (FEA), however, two of these motors (Mot1 and Mot2) are prototyped for further experimental comparison.

For all the motors, the peak conditions refers to a 10s overload, with a standard water jacket.

II. MOTOR COMPARISON

A first comparison between the motors can be directly done in Tab. I. Mot1 is the motor with higher torque and power, but also higher maximum speed (so potentially more structural issues), while the other motors have lower ratings (torque, power and maximum speed). The IPM motor is the one with

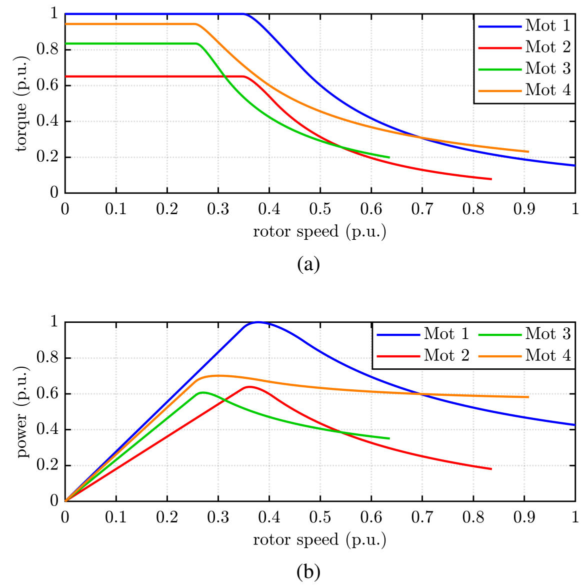

Fig. 2. Torque versus speed and power versus speed profiles of the four motors, normalized on the Mot1 specs.

the widest field-weakening region (ratio between maximum speed and base speed), as will be clarified and discussed later. Besides Mot3, the other motors have similar outer diameter, while the stack length is different for the three motors, with Mot2 that is the shortest and lightest one. Dealing with inverter ratings, Mot1 and Mot2 share the same DC link voltage, while the other two motors presents reduced DC link. About the current ratings, Mot1 and Mot4 have practically the same peak current, while the other two motors have reduced current. The overall inverter rating (apparent power) is different for the four motors, with Mot1 that have the biggest inverter and Mot4 the smallest one (in terms of apparent power). Before entering in the parameters normalization and Key Performance Index (KPI), the peak torque and power profiles at maximum inverter ratings are reported in Fig. 2.

As said, the ratings and curves of the four motors are different and reflects also the different technology and design choices. Mot4 has intermediate power and torque, but presents the widest field weakening area, thanks to the NdFeB PMs, while Mot1 and Mot2 have poor field-weakening capability. Among the four motors, Mot1 is the one with highest torque and power in absolute values. A last comment about the motor difference must be done on the winding technology: the first three motors are designed with hairpin windings, allowing a higher slot filling factor compared to Mot4, that have stranded winding. These differences in loss term, however, the cooling system of each motor is designed in order to survive for 10s in the peak conditions declared in Tab. I.

A. Maximum Speed and Field-Weakening Operation

The comparison in terms of maximum speed and field weakening performance is reported in Tab. II. For a clearer comparison, the power profiles of the four motors are reported

TABLE II
HIGH-SPEED REGION AND INVERTER RATINGS

	Mot1	**Mot2**	**Mot3**	**Mot4**
Max speed by base speed	2.91	2.41	2.51	3.59
Power at max speed by peak power	0.47	0.28	0.58	0.83
Maximum tip speed (m/s)	148	124	85	118
kW/kVA	0.64	0.51	0.64	0.77

in Fig. 3, normalized for the base speed and power of each motor.

The ratio between the maximum and base speed of the three motors is the first compared index. The ratios span between 2.4 (Mot2) to more than 3.5 (Mot4), according also to the motor technology. Besides the speed ratio, that represents the field-weakening speed range, an important KPI is the ratio between the power at maximum speed and the peak power, index of the actual field-weakening capability of the motor. The best design in this sense is Mot4 thanks to the NdFeB PMs that allows a high characteristic current (similar to the maximum current) and an almost flat power profile (less than 20% of power detriment at high speed). The two PM-SyRMs perform in a worse way, mainly because of the weak ferrite PMs that are not able to assist the field-weakening, because of the low resulting characteristic current. Furthermore, Mot1 is even more penalized by the thick structural ribs, that drain the PM flux, further reducing the characteristic current and the power at maximum speed and the higher speed compared to Mot3. Last, Mot2 presents the worst field-weakening operation because of the SyRM nature and presents a power drop between base speed and maximum speed of about 72%. This suggest that SyRMs are suitable as boost motors for low speed operations and not as main traction motors.

Furthermore, the ratio between output active peak power and inverter apparent power is reported in Tab. II. This term is important because it is related to the power factor of the motor and so the exploitation of the inverter limits for the power production. The two PM-SyRM have similar kW/kVA ratio, around 0.64, while the SyRM has a lower value, around 0.5 and the V-type IPM motor have the best ratio, around 0.77. It follows that, the SyRM needs a bigger inverter, compared to the PM-SyRM, since the PMs in the PM-SyRM structure are adopted to increase the power factor and improve the field weakening capability. However, the numbers of the

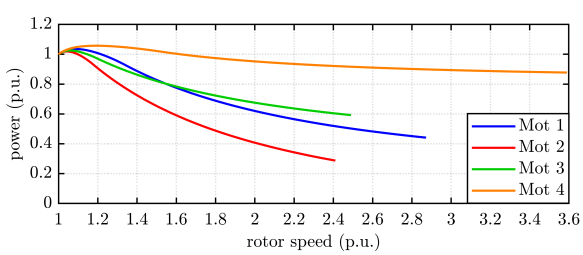

Fig. 3. Field-weakening performance comparison: power versus speed curves normalized to the base speed point for each motor

TABLE III
TORQUE AND POWER DENSITY

		Mot1	**Mot2**	**Mot3**	**Mot4**
Torque (peak)	(Nm/kg)	10.0	11.1	11.9	13.4
Power (peak)	(kW/kg)	6.2	6.8	5.4	6.2
Power (max speed)	(kW/kg)	2.6	1.9	3.1	5.1
Torque (peak)	(Nm/L)	62.9	64.2	81.6	87.1
Power (peak)	(kW/L)	39.1	39.1	37.0	40.2
Power (max speed)	(kW/L)	16.7	11.0	21.3	33.4

rare-earth-free motors have worst kW/kVA rating than the NdFeB-PMSM, so this comparison is important when system considerations are done.

The last comparison in terms of speed is the maximum tip speed that is the tangential speed at the rotor outer diameter and is directly related to the structural problems. As expected, Mot3 has a much smaller tip speed, because of the minimum maximum speed, but also because of the lower rotor diameter (smaller torque output).

B. Torque and Power Density

Torque and power densities are common KPIs for electric motors. In Tab. III the four motors are compared in terms of torque and power densities, both gravimetric and volumetric. It must be remarked that in this analysis, just the active part mass and volume is considered (shaft, housing, cooling system, sensors and inverter are disregarded).

As expected from the previous analysis, Mot4 is the one with best specific indicators, both in terms of torque and power. The interesting outsider is Mot2 (SyRM), that offers a very high peak power density, thanks to the relatively high speed, the high current density (because of the hairpin windings, as will be commented later) and the possibility to overload without demagnetization risk. Obviously, at maximum speed, Mot2 has the worst indicators among the motors. Dealing with torque density, Mot4 has the best Nm/kg index, thanks to the NdFeB PMs, but this KPI for the four motors is similar. The important difference between Mot4 and the other motors is the power density at high speed: thanks to the superior field-weakening performance, the power density at maximum speed is more than 60% higher than Mot3. The difference is even more pronounced if Mot1 (that have a similar maximum speed) is considered, with a factor of about 2 between the power densities at maximum speed of the two motors.

For a more complete assessment of the torque and power densities differences among the four motors, the torque and power densities profiles versus tip speed are reported in Fig. 4 and Fig. 5 for gravimetric and volumetric indexes, respectively. The tip speed, that is the linear speed at the periphery of the rotor, is selected as a general and independent indicator for motor speed. This comparison highlight some features of the compared motor. First of all, Mot1 and Mot2 shares the same base tip speed and it is worth noting that the SyRM higher gravimetric peak torque and power densities and practically the same volumetric torque and power densities.

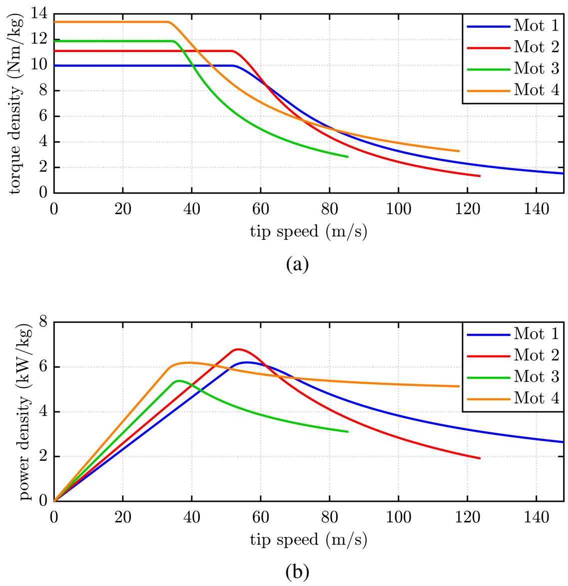

Fig. 4. Gravimetric torque and power densities versus tip speed profiles of the four motors.

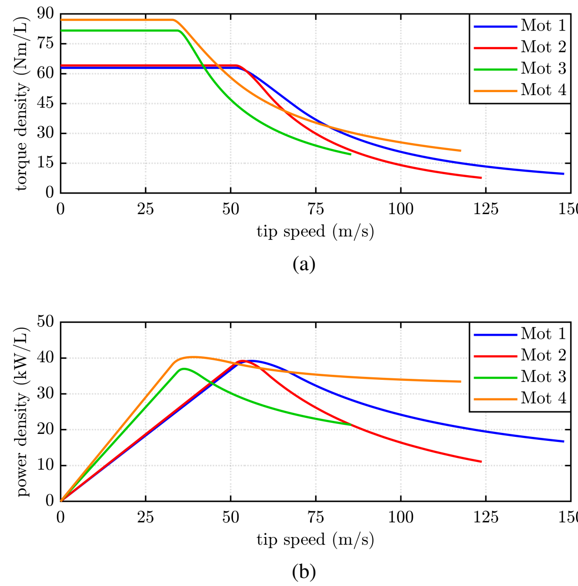

Fig. 5. Volumetric torque and power densities versus tip speed profiles of the four motors.

This is caused by a number of factors, but primarily by the higher maximum speed of the PM-SyRM, that request thicker structural ribs, nullifying the advantage of the PMs in terms of torque production. Another key difference is the possibility to overload the SyRM without the risk of demagnetization, allowing higher peak torque. Last, the gravimetric indexes favor the SyRM because of the lighter rotor (air in place of PMs). However, as said before, the field-weakening operation is quite different for the two motors, with the advantage of ferrite PMs that becomes significant against the SyRM solution, even if not optimal compared to NdFeB PMs. Dealing with the other motors, Mot3 and Mot4 shares the same base tip speed, but performs in a different way both in terms of peak conditions and in field-weakening operations, highlighting the advantages of the NdFeB PMs against ferrite. Furthermore, this comparison is in favor of the PM-SyRM, since Mot4 has a higher maximum tip speed, so a more critical structural design. Last interesting point is the fact that Mot4 presents the higher power density for almost all the speed range, with the only exception of the base speed of Mot1 and partially Mot2.

The effect of the maximum motor speed on the torque and power densities is reported in Fig. 6. Here is evident that, increasing the maximum speed, the torque density (both gravimentric and volumetric) decrease. Furthermore, Mot4 is out of this pseudo-curves because of the NdFeB PMs contribution. The inverse proportionality between torque density and maximum speed is mainly given by the thicker ribs, that drain more magnetic flux and worsen the PM effect. The SyRM can be compete with the PM-SyRMs just because of the higher current density.

Dealing with the power density, the data for both peak power and power at maximum speed are reported. About the peak power density, the four motors express similar power density, suggesting the fact that a limit is reached: increasing the

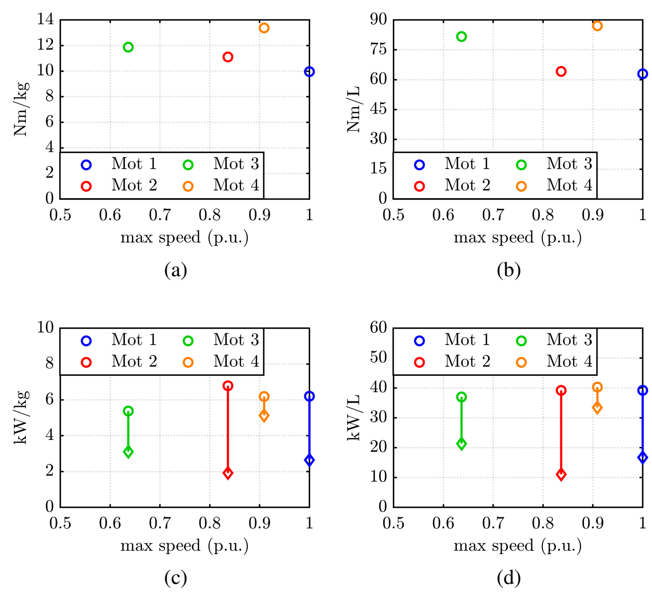

Fig. 6. Torque and power densities function of the maximum motor speed. Circle refers to peak condition and diamonds refers to max speed condition

speed will not lead to power density improvements, because of structural limits. The key difference here is with the power densities at maximum speed. In this case, the outstanding winner is Mot4 thanks to the NdFeB PMs. Moreover, the comparison between Mot1 and Mot3 highlights that increase the maximum speed of ferrite PMSMs have no advantages in terms of power density over the whole speed range.

C. Linear Current Density and Fault Reaction

The comparison of the four motors is extended to the linear current density, to investigate how different is the current loading of each motor. The comparison is reported in Tab. IV.

TABLE IV
LINEAR CURRENT DENSITY AND FAULT REACTION

		Mot1	Mot2	Mot3	Mot4
Peak current	(kA/m)	160	192	228	216
Demagnetization	(kA/m)	160	-	228	558
HWC current	(kA/m)	351	367	414	474
PM flux linkage	(%)	11%	-	21%	69%
UGO speed ratio	(p.u.)	3.18	-	1.95	0.41

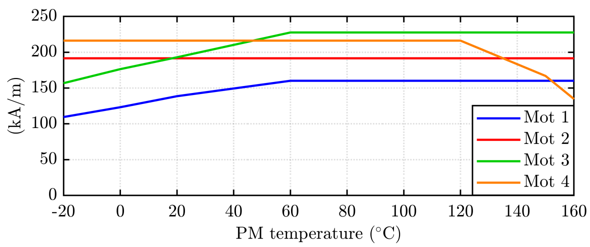

Fig. 7. Maximum allowed linear current density function of the PM temperature, according to inverter and demagnetization limits.

The first interesting point is the fact that the two PM-SyRM have the peak linear current density equal to the demagnetization limit. This means that if the current is slightly increased, the PMs will irreversibly demagnetize. This high current density helps to increase the torque and power densities, but pose the risk of irreversible demagnetization at low temperatures, in case of control issues and in case of faults. The maximum allowed linear current density is higher for Mot3 thanks to the higher PM content (in percentage), helping the torque density index of this motor compared to the other two prototypes. Mot4 have margin in demagnetization and a derating is expected just above 120°C. Mot2 has no demagnetization limits, so can have a higher linear current density compared to Mot1, with the only limit of the cooling system and no deratings in temperature. The maximum linear current density, given by inverter limit and demagnetization limit, is reported in Fig. 7.

It is worth noting that the linear current density derating at 0°C is about 23% for both PM-SyRM motors, that could be reflected in a torque and power derating of similar magnitude.

Dealing with fault condition [8], there are two possibles post-fault states: Open Circuit (OC) and Active Short-Circuit (ASC) [9]. The latter is preferred, since avoid the risk of harmful voltages. The issue is the peak current [10], that can demagnetize the PMs. The Hyper-Worst-Case (HWC) scenario is considered in Tab. IV, highlighting that the two PM-SyR will demagnetize if ASC is triggered. However, Mot4 can survive to ASC without irreversible demagnetization at its rated temperature. Last comment for ASC, it must be remarked that the SyRM presents high HWC current because of the rotor anisotropy, but there are no limitations dictated by demagnetization. For the fault reaction, the two PM-SyR can exploit the OC, since the PM flux linkage is quite small (11% and 21% of the rated flux linkage for Mot1 and Mot3, respectively), causing a small OC voltage at maximum speed. The Uncontrolled Generator Operation (UGO) speed is computed for the three PMSMs as the speed at which the no-load voltage equals the rated voltage. Above this speed, UGO will happens. This speed is expressed in Tab. IV as a ratio by the motor maximum speed, giving a quick index for the possible danger: for ratios higher than 1, the UGO speed will be higher than the maximum speed and UGO will not be a problem. The UGO speed results 3.18 and 1.95 times the maximum speed of Mot1 and Mot3 respectively, confirming that these to motors can work in OC without risk. On the other hand, UGO speed is less than half of the maximum speed of Mot4, making mandatory for the NdFeB PMSM the ASC strategy.

III. ENVIRONMENTAL IMPACT ASSESSMENT

To evaluate the environmental impact of the four motors, the Environmental Priority Strategy (EPS) indicator is adopted [6]. Based on the reference tables and the standard composition of the electric steel lamination, winding and PMs adopted, the EPS, measured in Environmental Load Units (ELU), is computed for the considered machines. The mass composition of the four motors is reported in Tab. V and Fig. 8a. As expected, the majority of the active mass of the motor is given by the laminations. From the composition in mass, it is evident that Mot1 is the one with lower content of copper, while Mot3 has the higher content of copper and PMs. Thanks to this feature, Mot3 can sustain higher current density than Mot1 with the same thermal limits and without increasing the demagnetization risk. Dealing with Mot4, it has the lowest percentage in mass of PMs, but the grade is completely different, both on electromagnetic side (as shown in the previous section) and on environmental impact point of view. The composition of the EPS index of each motor is reported in Fig. 8b. It is worth noting that, despite Mot4 presents the lowest content of PMs in mass (besides the SyRM), it presents also the higher value EPS, mainly because of the PMs. These alone contribute to about 40% of the EPS value of Mot4. For the other motors, the presence of ferrite PMs lower the PMs contribution of the EPS value to less than 1%, even if the PMs are more relevant in terms of mass. Besides Mot4, the EPS value of the PM-SyRMs and SyRM is given by the winding. A last comment should be done on Mot3, that, among the rare-earth-free motors, presents the highest ELU, slightly bigger than Mot1, but with reduced torque and power.

TABLE V
ACTIVE MASS AND EPS COMPOSITION

		Mot1	Mot2	Mot3	Mot4
PM mass	(%)	7.8%	0.0%	9.1%	4.9%
Winding mass	(%)	10.1%	12.6%	15.0%	13.7%
Lamination mass	(%)	82.1%	87.4%	75.9%	81.4%
PM EPS	(%)	0.6%	0.0%	0.5%	38.9%
Winding EPS	(%)	92.9%	94.4%	95.4%	58.1%
Lamination EPS	(%)	6.4%	5.6%	4.1%	3.0%

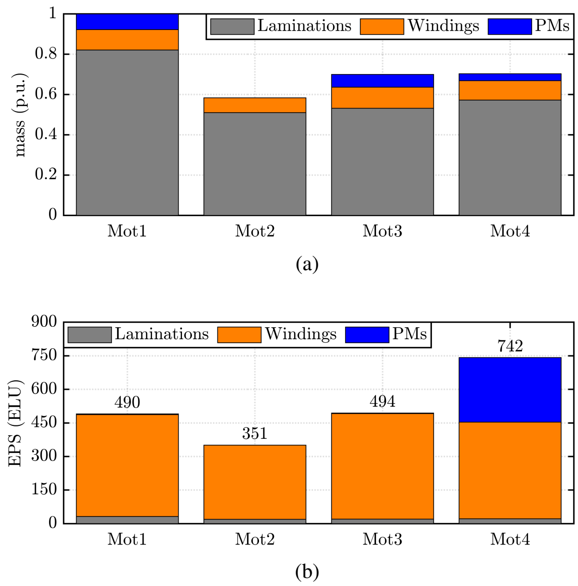

Fig. 8. Active mass part composition of the three motors and EPS index composition, based on active parts

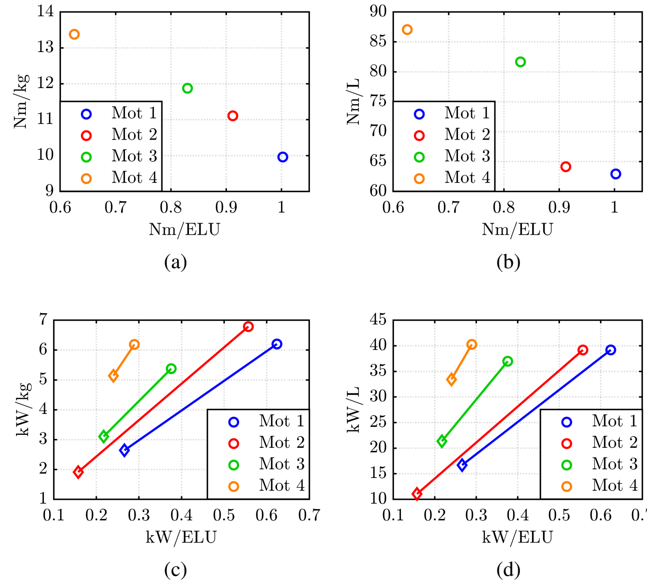

Fig. 10. Trade-off between torque and power densities (gravimetric and volumetric) and the specific torque and power per EPS

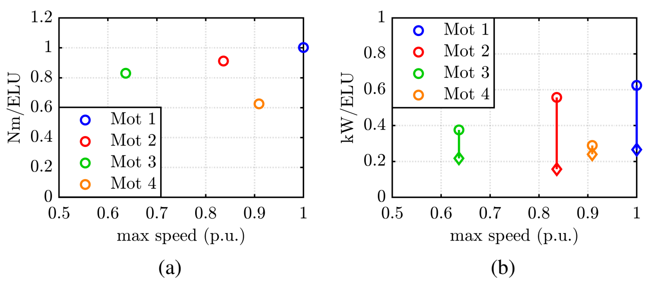

Fig. 9. Torque per EPS and power per EPS function of the motor maximum speed. Circle refers to peak condition and diamonds refers to max speed condition

A. Torque and Power per EPS Value

The specific torque and power per EPS are reported in Fig. 9 function of the maximum speed. From this analysis, Mot1 results the better performing, with higher peak torque and power per EPS, while, for the rare-earth-free motors, the torque and peak power density increase with the maximum speed. This could be related to the reduced winding content in percentage. In this comparison, Mot4 is completely out of the trend of the other motors, because of the NdFeB content, presenting lower Nm/ELU and kW/ELU values in peak conditions. Dealing with the power at maximum speed, the PMSMs are aligned to similar values with the best field-weakening operation of Mot4 that balance the high ELU value.

B. Specific Quantities Comparison

A final comparison can be done comparing the torque and power densities in mass, volume and EPS, as done in Fig. 10. Dealing with torque production, the four motors lies on a Pareto front. The best in terms of Nm/kg and Nm/L is Mot4 (NdFeB PMSMs), as expected, while the best in terms of environmental impact is Mot1, so ferrite PMSM at high speed and reduced copper content. The conclusion is different if the power production is considered. Dealing with the peak power, Mot1 and Mot2 are the best performing motors, lying both on the Pareto front, while Mot4 is included in the Pareto front just for the volumetric peak power density. However, if the power at maximum speed is considered, the dominant solutions are Mot1 and Mot4. These presents similar kW/ELU value, with the advantage of Mot4 on the gravimetric and volumetric density.

IV. Conclusions

Four motors for traction applications are compared in terms of specific KPIs. The four motors include standard traction motor with NdFeB PMs and rare-earth-free solutions as ferrite PM-SyRMs and SyRM. Besides the typical KPIs as torque and power density, also the environmental impact of the four motors is computed and adopted for the computation of specific indexes. From the comparison, it is evident that, on a power density point of view, the best motor is the one with NdFeB PMs, especially when the power on the whole speed domain is considered. Dealing with the peak performance, the interesting result is the high power density of the SyRM, given by the hairpin winding and the higher linear current density compared to the PM-SyRMs, that are limited by demagnetization limits. Considering the PM-SyRMs with ferrite PMs, one of the interesting result is the limited advantage given by the maximum speed increase because of the more critical structural design that further reduce the net PM flux linkage. In this case, the advantages of the PM-SyRM on the SyRM (designed for lower speed) are marginal. On the other hand, if the environmental impact is considered, the conclusion slightly changes. The high EPS value of the NdFeB PMs increase the index of SyRM and PM-SyRMs, at the cost of lower torque and power density. However, if the power on the whole speed range is considered, NdFeB PMs are still competitive with rare-earth-free solutions also on an environmental point of view.

Acknowledgment

The research has been conducted with the support of Power Electronics Innovation Center (PEIC) of Politecnico di Torino.

References

[1] A. Krings and C. Monissen, "Review and Trends in Electric Traction Motors for Battery Electric and Hybrid Vehicles," in *2020 International Conference on Electrical Machines (ICEM)*, vol. 1, Aug. 2020.

[2] W. Soong and N. Ertugrul, "Field-weakening performance of interior permanent-magnet motors," *IEEE Transactions on Industry Applications*, vol. 38, no. 5, pp. 1251–1258, 2002.

[3] A. El-Refaie and M. Osama, "High specific power electrical machines: A system perspective," *CES Transactions on Electrical Machines and Systems*, vol. 3, no. 1, pp. 88–93, 2019.

[4] P. Quassolo, F. Togni, E. Preci, and A. Acquaviva, "Design considerations for high power density traction pm motors with hairpin windings," in *2022 International Conference on Electrical Machines (ICEM)*, 2022, pp. 1669–1674.

[5] W. Feng, K. Chen, J. Paddock, T. Jahns, and B. Sarlioglu, "Design and comparison of surface inset permanent magnet machine and surface permanent magnet machine without heavy rare earth magnets for traction applications," in *2023 IEEE Energy Conversion Congress and Exposition (ECCE)*, 2023, pp. 4022–4029.

[6] "Environmental Priority Strategies (EPS)." [Online]. Available: https://www.ivl.se/english/ivl/our-offer/our-focus-areas/consumption-and-production/environmental-priority-strategies-eps.html

[7] P. Ragazzo, G. Dilevrano, S. Ferrari, and G. Pellegrino, "Design of ipm synchronous machines using fast-fea corrected design equations," in *2022 International Conference on Electrical Machines (ICEM)*, 2022, pp. 1–7.

[8] G. Choi and T. M. Jahns, "Investigation of key factors influencing the response of permanent magnet synchronous machines to three-phase symmetrical short-circuit faults," *IEEE Transactions on Energy Conversion*, vol. 31, no. 4, pp. 1488–1497, 2016.

[9] P. Ragazzo, G. Dilevrano, S. Ferrari, and G. Pellegrino, "Comparative turn-off safe modes of ferrite- and ndfeb- interior pmsms," in *2023 IEEE Energy Conversion Congress and Exposition (ECCE)*, 2023, pp. 4133–4139.

[10] S. Ferrari, G. Dilevrano, P. Ragazzo, P. Pescetto, and G. Pellegrino, "Fast determination of transient short-circuit current of pm synchronous machines via magnetostatic flux maps," *IEEE Transactions on Industry Applications*, vol. 59, no. 4, pp. 4000–4009, 2023.